Advances in Water Resources 53 (2013) 139–149

Contents lists available at SciVerse ScienceDirect

Advances in Water Resources

journal homepage: www.elsevier.com/locate/advwatres

# On the interpretation of hydraulic pulse tests on rock specimens

A.P.S. Selvadurai *, M. Najari

Department of Civil Engineering and Applied Mechanics, McGill University, 817 Sherbrooke Street West, Montréal, QC, Canada H3A 0C3

ARTICLE INFO

*Article history:*
Received 13 August 2012
Received in revised form 13 November 2012
Accepted 14 November 2012
Available online 29 November 2012

*Keywords:*
Hydraulic pulse tests
Biot poroelasticity
Grain compressibility
Pulse decay
Computational modeling
Analytical estimates

ABSTRACT

A widely used procedure for interpreting results of hydraulic pulse tests involves an analysis that is based on the piezo-conduction equation. In this paper, the range of applicability of the classical piezo-conduction equation is examined in the light of results derived from Biot's classical theory of poroelasticity, which takes into account complete coupling involving fluid flow and skeletal deformations along with influences of grain compressibility. Comparisons are made between the two approaches by considering typical low permeability rocks including Westerly Granite and Indiana Limestone, where the permeabilities can vary by orders of magnitude. These studies are complemented by experiments performed on samples of Stanstead Granite, the results of which were analyzed employing the different approaches.


## 1. Introduction

Permeability of geomaterials can be determined using either steady state or transient tests depending on the relative values of the anticipated permeability. For low permeability geomaterials, with permeabilities in the range $K \in (10^{-18}, 10^{-22})\,\mathrm{m}^2$, the accurately verifiable steady flow rates that can be initiated in unstressed samples without causing damage (e.g. micro-mechanical hydraulic fracture) to the porous fabric can be small. For this reason, fluid transport characteristics of low permeability geomaterials are usually determined from transient flow tests. The use of transient flow tests was pioneered by Brace et al. [1] and has been successfully used to estimate the permeability of most low permeability geomaterials. The theoretical expositions of the development of the piezo-conduction equation are given by other researchers [2–5] and relevant applications of the concepts are demonstrated by [6–11]. Hydraulic pulse tests referred to previously have largely focused on axial flow configurations. The procedures have also been applied in the area of well testing [12–15] and in laboratory testing of radial flows in cylinders [16–18]. Saturation of the geomaterial is an essential requirement for the conventional modeling of the hydraulic pulse test. With low permeability geomaterials, residual pressures can reside in a sample following a saturation sequence. The influence of such pressure artifacts on the interpretation of hydraulic pulse tests has been examined by Selvadurai [19].

The development of the theory for the piezo-conduction equation is carried out by imposing certain restrictions on the mechanical response of the porous skeleton of the geomaterial. For example, the theory can only account for compressibility of the porous skeleton and that of grains composing the porous skeleton. A more accurate development of fluid pressure decay in pulse tests should take into consideration the influence of *complete coupling* between a deformable porous skeleton and a compressible permeating fluid. An example is the classical theory of poroelasticity proposed by Biot [20] that takes into consideration elastic deformations of the porous skeleton, the compressibility of the material composing the porous skeleton and Darcy flow in the connected pore space. The possible influences of the two approaches for examining the results of hydraulic pulse tests on the interpretation of permeability values have led to comparative investigations and two examples are provided by Walder and Nur [21] and Hart and Wang [22] (see also Wang [23]). Both investigations deal with hydraulic pulse tests conducted under one-dimensional conditions with the first investigating the poroelastic phenomena including a non-linear pore pressure diffusion associated with large pore pressure gradients and the latter considering the three-dimensional poroelastic influences that arise when modeling the one-dimensional hydraulic pulse tests. It should also be noted that the problem examined by Hart and Wang [22] relates to computational modeling of the propagation of a hydraulic pulse to a one-dimensional element that is hydraulically sealed at all surfaces other than at the region subjected to pressure.

The objectives of the paper are as follows: (i) re-examine the axial flow and radial flow hydraulic pulse tests in the context of the piezo-conduction analyses (analytical) and the fully coupled

* Corresponding author.
*E-mail addresses:* patrick.selvadurai@mcgill.ca (A.P.S. Selvadurai), meysam.najari@mail.mcgill.ca (M. Najari).

0309-1708/$ - see front matter © 2012 Elsevier Ltd. All rights reserved.
http://dx.doi.org/10.1016/j.advwatres.2012.11.008

theory of poromechanics (computational), (ii) evaluate the distinctions that arise between the two approaches when the approaches are used to examine hydraulic pulse tests that have been reported in the literature (e.g. Indiana Limestone and Westerly Granite), and (iii) use the two modeling approaches to interpret the permeability characteristics of Stanstead Granite (Stanstead, QC, Canada) by examining results of radial flow permeability tests and to use the estimates for permeability to predict the pulse decay test conducted at a circular patch located on the surface of a cylindrical sample of Stanstead Granite.

## 2. Governing equations

The partial differential equations governing coupled fluid flow and linear elastic deformation of a fluid saturated isotropic porous medium were developed by Biot [20]. The theory is well documented in the literature and alternative expositions and representations of Biot's theory are also presented in a number of key articles including [24–27]. Reviews of the subject of isothermal poroelasticity are also given in [28–33]. The classical theory of poroelasticity takes into account Hookean isotropic elastic deformation of the porous skeleton, the elastic deformation of the solid material composing the porous skeleton, the compressibility of the pore fluid and fluid flow behavior, which is characterized by Darcy's law. The dependent variables in the formulation consist of the skeletal deformation $\mathbf{u}(\mathbf{x},\ t)$ and the pore fluid pressure $p(\mathbf{x},\ t)$ ($p > 0$ for compressive pore fluid pressure), where $\mathbf{x}$ is the position vector and $t$ is time. Considering only quasi-static processes, the governing fully coupled partial differential equations take the form

$$G\nabla^2\mathbf{u} + \left(K_{eff} + \frac{G}{3}\right)\nabla(\nabla\cdot\mathbf{u}) - \alpha\nabla p = 0 \qquad (1)$$

$$\frac{K}{\mu}\nabla^2 p - S^*\frac{\partial p}{\partial t} - \alpha\frac{\partial}{\partial t}(\nabla\cdot\mathbf{u}) = 0 \qquad (2)$$

where $G$ and $K_{eff}$ are, respectively, the shear modulus and the bulk modulus of the porous skeleton, $K$ is the permeability, $\mu$ is the dynamic viscosity of the fluid and $S^*$ and $\alpha$ are, respectively, a storativity term and the *Biot coefficient* defined by

$$S^* = nC_w + (\alpha - n)C_s, \quad \alpha = \left(1 - \frac{C_s}{C_{eff}}\right) \qquad (3)$$

The partial differential equation governing flow of a compressible fluid through the accessible pore space of a porous medium with a skeletal compressibility $C_{eff}$ (i.e. the inverse of $K_{eff}$) and a grain compressibility $C_s$ was derived by Brace et al. [1] and takes the form

$$\frac{K}{\mu}\nabla^2 p = S_B\frac{\partial p}{\partial t} \qquad (4)$$

where

$$S_B = \{nC_w + C_{eff} - (n+1)C_s\} \qquad (5)$$

When $C_s$ reduces to zero, Eq. (5) reduces to the conventional storativity term and gives rise to the piezo-conduction equation used quite extensively in the interpretation of permeability in geohydrological problems [2,3,5,19]; i.e.

$$S_C = [nC_w + C_{eff}] \qquad (6)$$

At the outset, it should be mentioned that the fully coupled theory of poroelasticity requires the formulation of the initial boundary value problem with precise conditions relevant to an experimental configuration, where consistent initial and boundary conditions are applied to all the dependent variables. The solution of the conventional piezo-conduction equation requires the formulation of an initial boundary value problem where consistent initial and boundary conditions are prescribed only on the single dependent variable, namely the pore fluid pressure.

## 3. Theoretical modeling

In this section we present, for completeness, the solution to the initial boundary value problem governing hydraulic pulse tests conducted under one-dimensional and radially symmetric conditions.

### 3.1. Analytical results

The piezo-conduction equation of the type (4) can be examined for relatively simple geometries involving axial, radially symmetric and spherically symmetric flow conditions. In the case of purely axial diffusion of a pressure pulse applied to a fluid chamber of volume $V_w$ in contact with the boundary of a semi-infinite fluid saturated region, the initial boundary value problem has been investigated quite extensively (see [19] for a presentation of the relevant literature) and it is sufficient to record the relevant boundary and initial conditions applicable to a semi-infinite domain. These are

$$p(0,t) = \bar{p}(t); \quad \bar{p}(0) = \bar{p}_0 \qquad (7)$$

$$\Phi\left(\frac{\partial p}{\partial z}\right)_{z=0} = \left(\frac{\partial p}{\partial t}\right)_{z=0} \qquad (8)$$

$$p(z,0) = 0 \qquad (9)$$

where $\bar{p}(t)$ is the position independent fluid chamber pressure, which is a function of time only and $\bar{p}_0$ is the chamber pressure at the start of the axial flow pulse test and

$$\Phi = \left(\frac{AK}{\mu V_w C_w}\right) \qquad (10)$$

In Eq. (10) $A$ is the cross-sectional area of the one-dimensional semi-infinite domain and $V_w$ is the volume of the pressurized reservoir used in the test. One-dimensional pulse tests are invariably conducted on low permeability materials of finite extent and it is usually assumed that the far-field boundary has a limited influence on the observed pulse decay. If this condition is satisfied, the solution to the piezo-conduction equation should also satisfy the regularity condition, $p(z,\ t) \to 0$ as $z \to \infty$. The extent to which the assumption of 'infinite extent' is valid for a finite sample tested in the lab was analytically examined by Selvadurai and Carnaffan [16] (it is not a requirement that this far field condition be satisfied [9]; its inclusion, however, leads to a simplified result applicable to a semi-infinite domain). Considering the above, the solution of the initial boundary value problem can be expressed in the non-dimensional form

$$\frac{\bar{p}(t)}{\bar{p}_0} = \exp(\Omega^2 t)\ \mathrm{Erfc}(\sqrt{\Omega^2 t}) \qquad (11)$$

where

$$\Omega = \Phi\omega, \quad \omega^2 = \frac{S_i\mu}{K} \qquad (12)$$

and the storativities $S_i$ can be given values $S_B$ and $S_C$ that correspond to the expressions (5) and (6), respectively.

A similar analysis can be applied to examine the purely radial flow hydraulic pulse tests conducted through the pressurization of a borehole located in a fluid saturated porous medium of infinite extent over a borehole length $H$, containing the fluid volume $V_w$. The details of the analysis are given in [12–14]. Applications of the radial flow technique to the measurement of permeability characteristics of a cement grout cylinder measuring 152 mm in diameter and granite cylinders measuring 450 mm in diameter are given, respectively, in the articles by Selvadurai and Carnaffan [16] and Selvadurai et al. [17]. More recently, Selvadurai and Jenner [18] used the radial flow pulse test to determine the permeability characteristics of a very low permeability argillaceous Lindsay-Cobourg Limestone ($K \in (10^{-22}$ to $10^{-19}\ \mathrm{m}^2)$). The boundary conditions and initial conditions applicable to the purely radial flow problem are

$$p(a,t) = \tilde{p}(t); \quad \tilde{p}(0) = \tilde{p}_0 \tag{13}$$

$$\frac{2\pi a K H}{\mu}\left(\frac{\partial p}{\partial r}\right)_{r=a} = V_w C_w \left(\frac{\partial p}{\partial t}\right)_{r=a} \tag{14}$$

$$p(r,0) = 0 \tag{15}$$

where $\tilde{p}(t)$ signifies the position independent cavity pressure and $\tilde{p}_0$ is pressure in the cavity at the start of the radial flow pulse test. In addition, if the modeling is applicable to an infinite domain the pressure field should satisfy the regularity condition, $p(r, t) \to 0$ as $r \to \infty$. The decay of the pressure within the cavity is given by

$$\frac{\tilde{p}(t)}{\tilde{p}_0} = \frac{8\tilde{\alpha}}{\pi^2}\int_0^\infty \frac{\exp(-\tilde{\beta}u^2/\tilde{\alpha})}{u f(u,\tilde{\alpha})} du \tag{16}$$

where

$$f(u,\tilde{\alpha}) = [uJ_0(u) - 2\tilde{\alpha}J_1(u)]^2 - [uY_0(u) - 2\tilde{\alpha}Y_1(u)]^2 \tag{17}$$

$J_0$ and $J_1$ are, respectively, the zeroth-order and first-order Bessel functions of the first kind and $Y_0$ and $Y_1$ are, respectively, the zeroth-order and first-order Bessel functions of the second kind. Also, in Eq. (16), the non-dimensional parameters $\tilde{\alpha}$ and $\tilde{\beta}$ are given by

$$\tilde{\alpha} = \frac{\pi a^2 H S_i}{C_w V_w}; \quad \tilde{\beta} = \frac{\pi K H t}{\mu V_w C_w} \tag{18}$$

Similarly, $S_i$ can be assigned the expressions defined by Eqs. (5) and (6).

## 4. Computational modeling

The analytical treatment of the initial boundary value problem in Biot's theory of poroelasticity associated with the one-dimensional axial flow and radial flow pulse tests is non-routine and to the authors' knowledge there are no analytical results that examine the pulse decay effects, which incorporate fully coupled influences of poromechanics. For this reason, the fully coupled analysis of the one-dimensional axial flow and purely radial flow pulse tests is conducted using a computational technique. Finite element modeling of problems in poroelasticity is well established and consistent formulation of initial boundary value problems is described by Lewis and Schrefler [26]; these procedures have also been implemented in several computational codes including ABAQUS™ and COMSOL™.

Detailed calibration exercises involving the COMSOL™ code are presented by Selvadurai and Suvorov [34,35] and Selvadurai et al. [36]. In these studies, the accuracy of the computational algorithms for coupled transient problems has been validated through comparisons with either known or newly developed analytical solutions. The axial hydraulic pulse test was first examined using a one dimensional axisymmetric domain as shown in Fig. 1. The figure shows a fluid saturated porous region of radius $a$ and length $l = 30a$. The domain of the porous region is $r \in (0, a)$; $z \in (0, l)$ and the plane boundary $z = 0$; $r \in (0, a)$ is in contact with a fluid reservoir of volume $(0.01\pi)a^3$ for Westerly Granite and $(0.4\pi)a^3$ for Indiana Limestone. The external boundary of the reservoir is non-deformable and encloses a fluid volume $V_w$. The computational modeling of the one-dimensional hydraulic pulse test can be developed considering two approaches: (a) the *state of stress* is assumed to be one-dimensional (Fig. 1) or (b) the *state of strain* is assumed to be one-dimensional (Fig. 2). In addition, the pore fluid pressure boundary condition should satisfy the no-flow boundary condition on the cylindrical surfaces of the one-dimensional domain. For the case (a), the boundary conditions applicable to the stresses, displacements and pore fluid pressures are

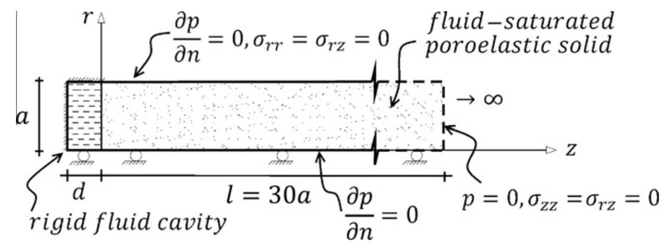


**Fig. 1.** Geometry and boundary conditions assumed for the one-dimensional stress hydraulic pulse test.

$$\begin{aligned}
&\sigma_{zz}(r,0,t) = 0; \quad u_r(0,z,t) = 0\\
&\sigma_{zz}(r,l,t) = 0; \quad u_z(r,0,t) = 0\\
&\sigma_{rz}(r,0,t) = 0\\
&\sigma_{rz}(a,z,t) = 0\\
&\sigma_{rz}(r,l,t) = 0\\
&\sigma_{rr}(a,z,t) = 0\\
&\left(\tfrac{\partial p}{\partial r}\right)_{r=a} = 0; \qquad p(r,l,t) = 0
\end{aligned} \tag{19}$$

In addition, the initial conditions correspond to

$$\mathbf{u}(r,z,0) = 0; \quad p(r,z,0) = 0 \tag{20}$$

The hydraulic pulse test is initiated by the application of a pressure pulse to the reservoir with a rigid boundary in contact with the poroelastic medium. If the domain of the reservoir is denoted by $\Omega_R$, the pore fluid pressure boundary condition at the reservoir and reservoir–poroelastic medium interface are given by

$$p(r,z,0) = \bar{p_0} \tag{21}$$

where $p_0$ is the pressure in the reservoir at the start of the pulse test.

Similarly, for the pulse test conducted under the one-dimensional strain condition the boundary conditions corresponding to Eq. (19) are

$$\begin{aligned}
&\sigma_{rz}(r,0,t) = 0; \quad u_r(0,z,t) = 0\\
&\sigma_{rz}(a,z,t) = 0; \quad u_r(a,z,t) = 0\\
&\sigma_{rz}(r,l,t) = 0; \quad u_z(r,0,t) = 0\\
&\sigma_{zz}(r,l,t) = 0\\
&\left(\tfrac{\partial p}{\partial r}\right)_{r=a} = 0; \qquad p(r,l,t) = 0
\end{aligned} \tag{22}$$

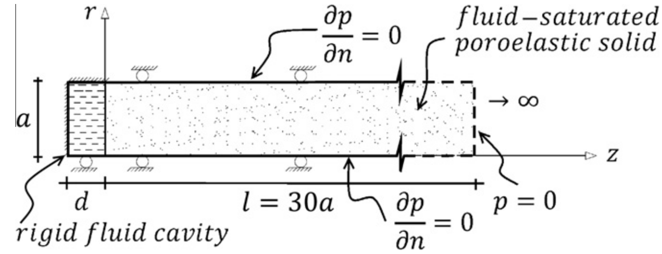


**Fig. 2.** Geometry and boundary conditions assumed for the one-dimensional strain hydraulic pulse test.

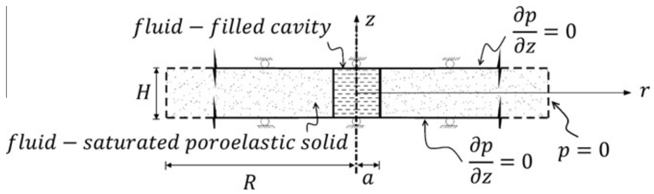


**Fig. 3.** Schematic view for the radially symmetric hydraulic pulse testing of an infinitely extended rock mass.

The initial conditions for the hydraulic pulse test conducted under one-dimensional strain are identical to Eq. (20) and the pulse test is initiated by a condition similar to Eq. (21).

Purely radial pulse testing was also examined (Fig. 3). The modeled element has a fluid cavity radius of $a$ and a height of $H = 20a$ for Westerly Granite and $H = 0.5a$ for Indiana Limestone. Unlike the one-dimensional model, here the size of the cavity can change due to cavity pressure changes. The corresponding boundary conditions are:

$$\begin{aligned}
&\sigma_{rr}(0,z,t) = 0; && \sigma_{rz}(0,z,t) = 0\\
&\sigma_{rr}(R,z,t) = 0; && \sigma_{rz}(R,z,t) = 0\\
&u_z(r,-H/2,t) = 0; && u_z(r,H/2,t) = 0\\
&u_r(0,z,t) = 0 && \\
&p(R,z,t) = 0; && \left(\tfrac{\partial p}{\partial r}\right)_{r=0} = 0\\
&\left(\tfrac{\partial p}{\partial z}\right)_{z=-H/2} = 0; && \left(\tfrac{\partial p}{\partial z}\right)_{z=H/2} = 0
\end{aligned} \tag{23}$$

The initial conditions for the purely radial flow pulse test are again identical to Eq. (20) and the initiating pressure is

$$p(r,z,0) = \tilde{p}_0 \tag{24}$$

To further establish the accuracy of the fully coupled poroelastic modeling of the hydraulic pulse test, the computational approach was applied to examine the one-dimensional problem that was examined by Hart and Wang [22]. The problem involves a cylinder measuring 0.0254 m in radius and 0.0309 m in height. The sample was sealed at the base and at the circumference such that no water flow could take place through these surfaces. The upper surface ($r \in (0,a)$; $z = l$) was subjected to a unit constant pore pressure pulse and the whole specimen was under constant total stress for the duration of the experiment. Fig. 4 shows the geometry and boundary conditions of the problem. The rock used was Berea Sandstone with hydro-mechanical parameters as follows [22,23]: the skeletal Young's modulus ($E$) = 13 (GPa); the skeletal Poisson's ratio ($\nu$) = 0.17; Biot coefficient ($\alpha$) = 0.764; permeability ($K$) = $1.91 \times 10^{-19}$ (m$^2$); porosity ($n$) = 5%; dynamic viscosity of water at 20 °C ($\mu$) = 0.001 (Pa s); density of water ($\rho$) = 1000 (kg/m$^3$); compressibility of water ($C_w$) = $4.35 \times 10^{-10}$ (Pa$^{-1}$). The test problem was modeled for a duration of 2500 s. The boundary and initial conditions used by Hart and Wang [22], who employed the ABAQUS™ code, are as follows:

$$\begin{aligned}
&\sigma_{rr}(a,z,t) = 0; && \sigma_{rz}(a,z,t) = 0\\
&\sigma_{zz}(r,0,t) = 0; && \sigma_{rz}(r,0,t) = 0\\
&\sigma_{zz}(r,l,t) = 0; && \sigma_{rz}(r,l,t) = 0\\
&u_r(0,z,t) = 0; && u_z(r,0,t) = 0\\
&\left(\tfrac{\partial p}{\partial r}\right)_{r=a} = 0; && z \in (0,l)\\
&\left(\tfrac{\partial p}{\partial z}\right)_{z=0} = 0; && r \in (0,a)
\end{aligned} \tag{25}$$

The identical boundary conditions were specified in the current analysis, which was performed using the COMSOL™ code. Fig. 4 also shows a comparison between the results obtained by Hart and Wang [22] and the current investigation; there is good correlation between the two sets of data. A detail of the short term pressure response at the sample end (i.e. $z = 0$) is also shown. This figure also illustrates, for purposes of comparison, the results obtained from the piezo-conduction equation presented by Hart and Wang [22] along with the results of the piezo-conduction modeling that (i) takes into consideration the influence of grain compressibility and (ii) that omits grain compressibility. For purposes of reference, we note that the piezo-conduction equation is also modeled using COMSOL, although an analytical solution can be developed using standard procedures (see e.g. [5,9,37]). The general observation arising from the computational modeling of the one-dimensional pulse test is that the influence of poromechanical coupling manifests only in the very early stages of the pulse response; this is characteristically similar to the Mandel–Cryer effect that gives rise to an increase in the pore pressure response due to skeletal deformations that produce an additional strain [38–41]. Also, when poromechanical coupling is omitted, the Mandel–Cryer effect does not materialize. In terms of the relevance of the observation to the interpretation of hydraulic pulse tests, it could be noted that the results of pulse tests in the very early stages of the pulse decay should not be used to estimate permeability. Similarly, the piezo-conduction equation modeling with a storativity term that includes effects of grain compressibility is expected to closely correlate with the results of the fully coupled modeling involving Biot poroelasticity. The results of hydraulic pulse test conducted on low permeability geomaterials can be ex-

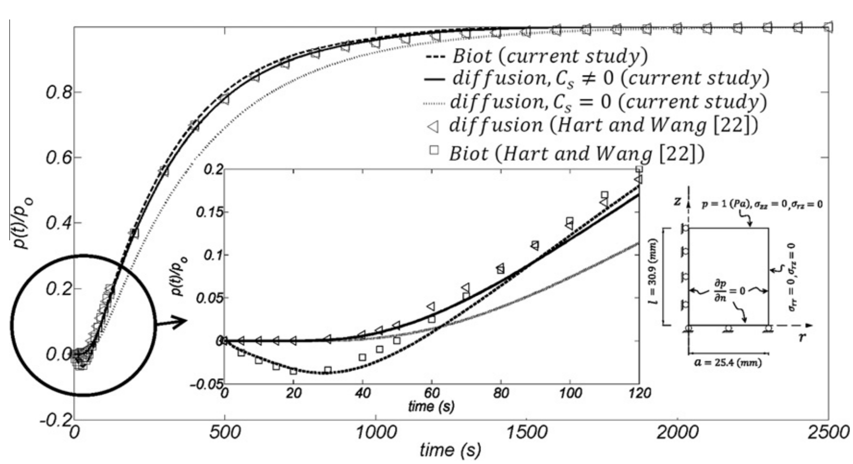


**Fig. 4.** Comparison of the results obtained by Hart and Wang [22] with the results of the current study. The figure also shows the detail of the initial 120 s and the geometry and boundary conditions of the problem.

**Table 1**
The mechanical, physical and hydraulic parameters applicable to Westerly Granite and Indiana Limestone.

| Rock type | $E$ (GPa) | $\nu$ | $\alpha$ | $K$ ($m^2$) | $n$ (%) |
|---|---|---|---|---|---|
| Westerly Granite[a] | 37.5 | 0.25 | 0.47 | $4.0 \times 10^{-19}$ | 1.0 |
| Indiana Limestone[b] | 24 | 0.14 | 0.85 | $73.75 \times 10^{-15}$ | 16.6 |

[a] Wang [23].
[b] Selvadurai and Selvadurai [45].

pected to produce differing responses depending on (i) the use of fully coupled analyses, (ii) the piezo-conduction equation that uses the conventional definition of storativity that includes compressibilities of the pore fluid and the porous skeleton, (iii) the piezo-conduction equation that takes into consideration the definition of storativity that includes fluid compressibility, skeletal compressibility and grain compressibility, and (iv) the state of deformation and flow associated with the hydraulic pulse test (i.e. axial flow, one-dimensional tests, radial flow well tests, etc.).

In order to examine the relative influences of factors (i)–(iv) on the results of pulse tests, computational simulations were carried out for hypothetical hydraulic pulse tests conducted on typical rocks such as Westerly Granite and Indiana Limestone. The input data used in the computational simulations is given in Table 1. Table 2 shows the values for the compressibilities and storativity terms used in the model. The computational results for the one-dimensional and radial flow hydraulic pulse tests were conducted using the boundary conditions and initial conditions defined by Eqs. (19)–(25). Fig. 5 shows the mesh configuration used in the axial and radial flow models. The interface between the fluid cavity and the rock was modeled using a very fine mesh to account for the Heaviside step function-type discontinuous pressure gradients that will be present at the start of the test, when the pore fluid pressure in the saturated geomaterial is set to zero everywhere within the porous medium. A Lagrange-quadratic element was used in the finite element model.

Figs. 6 and 7 illustrate respectively the computational results for one-dimensional and radial flow hydraulic pulse tests conducted on Westerly Granite and Indiana Limestone.

The following observations can be made, although these are not to be interpreted as results of a general nature.

### 4.1. One dimensional tests

(i) The results for hydraulic pulse tests conducted under one-dimensional states of stress and strain and incorporating Biot's fully coupled theory of poromechanics give very close results for one-dimensional Westerly Granite and relatively close results for the Indiana Limestone (maximum discrepancy of 1.3%).

(ii) The piezo-conduction equation analysis that also incorporates the influence of grain compressibility provides a closer correlation to results obtained from a Biot poroelastic analysis with a one-dimensional stress condition. This is not an unexpected result since the fully coupled Biot model takes into account the influence of grain compressibility through the inclusion of the $\alpha$ parameter.

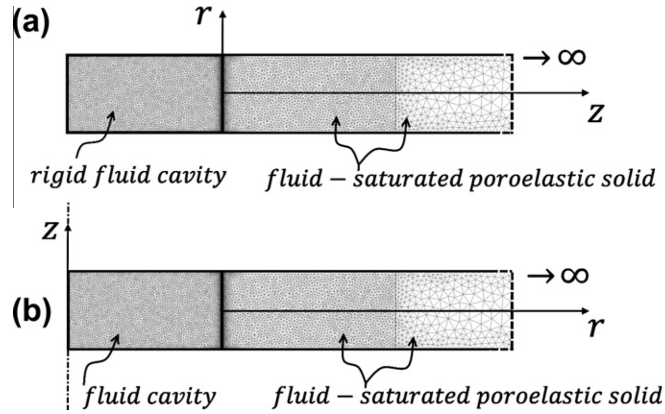


**Fig. 5.** Mesh configuration for modeling: (a) one-dimensional hydraulic pulse test (25,028 elements) and (b) radially symmetric hydraulic pulse test (30,017 elements).

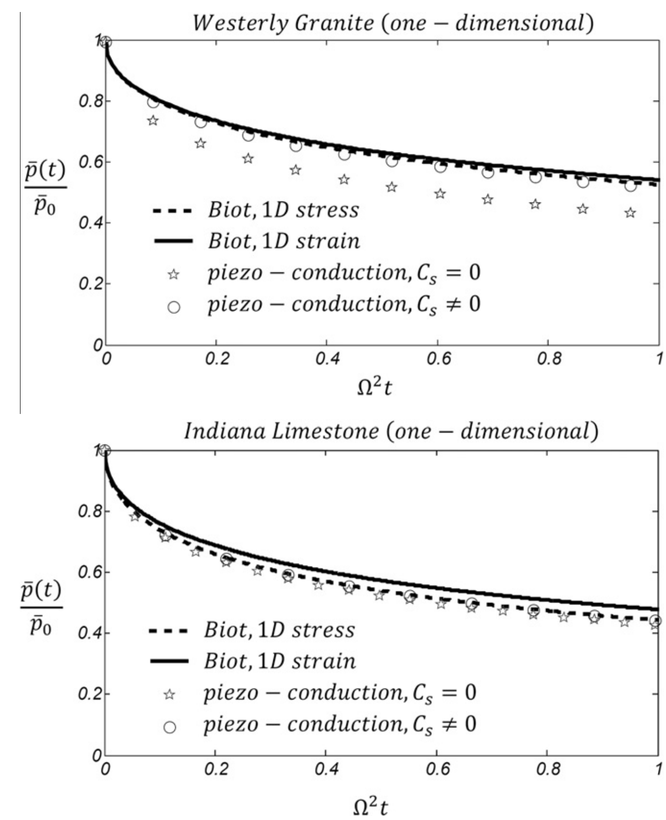


**Fig. 6.** Comparison of the pressure decay curves obtained from Biot's theory of poroelasticity with those obtained using the piezo-conduction equation for the one-dimensional hydraulic pulse test.

(iii) The pulse decay obtained from conventional hydraulic pulse test modeling (i.e. no poromechanical coupling and no influence of grain compressibility) shows a faster decay in the pressure pulse. This would imply an over estimation of the permeability. For example, if the one-dimensional result

**Table 2**
Storativity terms[a] for Westerly Granite and Indiana Limestone.

| Rock type | $C_{eff}$ ($Pa^{-1}$) | $C_s$ ($Pa^{-1}$) | $S^a$ ($Pa^{-1}$) | $S_P$ ($Pa^{-1}$) | $S_C$ ($Pa^{-1}$) |
|---|---|---|---|---|---|
| Westerly Granite | $4.00 \times 10^{-11}$ | $2.12 \times 10^{-11}$ | $1.43 \times 10^{-11}$ | $2.31 \times 10^{-11}$ | $4.45 \times 10^{-11}$ |
| Indiana Limestone | $9.00 \times 10^{-11}$ | $1.35 \times 10^{-11}$ | $8.46 \times 10^{-11}$ | $1.50 \times 10^{-10}$ | $1.65 \times 10^{-10}$ |

[a] In all estimates for $S$, the compressibility of water is taken as $4.54 \times 10^{-10}$ ($Pa^{-1}$) (White [44]).

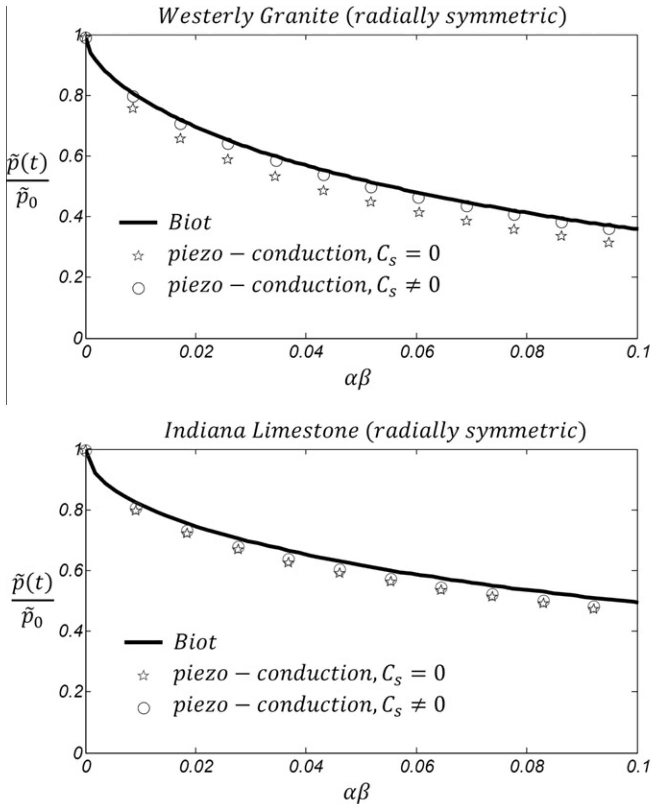


**Fig. 7.** Comparison of the pressure decay curves obtained from Biot's theory of poroelasticity with those obtained using the piezo-conduction equation for a radially symmetric hydraulic pulse test.

for Westerly Granite shown in Fig. 6 is chosen and the Biot results are considered a true representation, the permeability estimated from a piezo-conduction equation (without grain compressibility) needs to be reduced by approximately 58.5% to match the Biot results.

### 4.2. Radial flow tests

(i) In general, the radial flow hydraulic pulse tests are less influenced by fully poroelastic coupling when compared to the one-dimensional axial flow hydraulic pulse tests. The results for the fully coupled poroelastic hydraulic pulse decay compare favorably with the piezo-conduction equation results that incorporate grain compressibility.
(ii) The result from the conventional piezo-conduction equation analysis tends to over-estimate the permeability of the medium.

There is no simple non-dimensional parameter that would allow an identification of the discrepancy that might be expected between the fully coupled analysis and the conventional piezo-conduction equation analysis (with or without consideration of grain compressibility). It would appear that the discrepancies between the fully coupled analysis of the hydraulic pulse test and the result derived from the conventional piezo-conduction equation with storativity defined by Eq. (6) will become noticeable as the permeability of the material decreases.

### 4.3. Effect of aspect ratio

It is well known that under certain conditions the pressure diffusion equation (i.e. Eq. (2)) decouples from the skeletal deformation (i.e. $\alpha\frac{\partial}{\partial t}(\nabla\cdot\mathbf{u})\rightarrow 0$). Two of these conditions are the irrotational displacement in the finite or semi-finite domains (e.g. radially symmetric hydraulic pulse testing in an infinite medium) and the limit of the relatively compressible pore fluid [27]. It should, however, be noted that in such limiting cases the pore pressure decay obtained from the piezo-conduction equation is not equal to that obtained from Biot's poroelasticity formulation, since the estimate for storativity are different in the two formulations. The effect of the sample dimensions on the coupling parameters in Biot's poroelasticity has been studied by a number of researchers [27,42]. Since slender samples were utilized in the previously cited computational treatments, the influence of the aspect ratio on the decay of the hydraulic pulse was briefly investigated. The size of the cavity was kept constant for both one-dimensional and radial flow hydraulic pulse tests and either the length or the outer radius of the porous domain was changed. The hydraulic pulse tests were modeled for different sample sizes using the linear equations of poroelasticity and also for the piezo-conduction equation, with or without taking into account the compressibility of solid grains. The problem was modeled for each geometry for the first 50% reduction in the cavity pressure obtained from Biot poroelasticity formulation and then re-examined using the piezo-conduction equation over the same time duration. Finally, the cavity pressure at the end of each modeling exercise was compared with the poroelasticity solution to obtain the percentage error ($\delta(\%) = 100\times(p^{p-c} - p^{Biot})/p^{Biot}$) in the estimation of cavity pressure using the piezo-conduction equation. Figs. 8 and 9 show the calculated percentage error for, respectively, the one-dimensional and radially symmetric hydraulic pulse tests. It is evident that for both one-dimensional and radially symmetric problems the piezo-conduction equation provides results close to Biot's poroelasticity solution and, for smaller aspect ratios, the discrepancy between the results obtained from the two solutions becomes negligible.

## 5. Hydraulic pulse tests on Stanstead Granite

In this section we use the developments presented in the previous sections to examine the results of hydraulic pulse tests conducted on Stanstead Granite. The Stanstead Granite is described as a light gray coarse textured granite with grain sizes that range from 1 mm to 5 mm. The geomechanical properties of the Stanstead Granite were measured in the current study and compared with the studies by Iqbal and Mohanty [43]. The parameters used in the modeling were as follows: drained Young's modulus ($E'$) = 56 (GPa); drained Poisson's ratio ($\nu'$) = 0.13 (measured in accordance with ASTM D7012-04); Biot coefficient ($\alpha$) = 0.44; porosity ($n$) = 0.5–1.26% (measured in accordance with ASTM D4404-84); dynamic viscosity of water at 20 °C ($\mu$) = 0.001 (Pa s) [44]; density of water ($\rho$) = 1000 (kg/m$^3$); compressibility of water ($C_w$) = $4.54\times10^{-10}$ (Pa$^{-1}$) [44]. The value of the dynamic viscosity ($\mu$) was adjusted to account for the actual water temperature recorded for each test [44]. Two types of hydraulic pulse tests were conducted on the granite. The first involved pulse testing cylindrical samples of the granite under purely radial flow conditions and the second used a patch pulse test.

The cylindrical samples used in the experimental investigations measured 15.24 cm in diameter and 14.76 cm in height. The cylindrical surfaces of the samples were cored from a larger sample and the plane ends were machined smooth to accommodate a sealing gasket. The central cavity was prepared using a 2.54 cm diameter diamond drill and the surface of the cavity was air-blown to remove any debris that might be embedded on the surface of the cavity that could impede fluid flow by clogging the pore space.

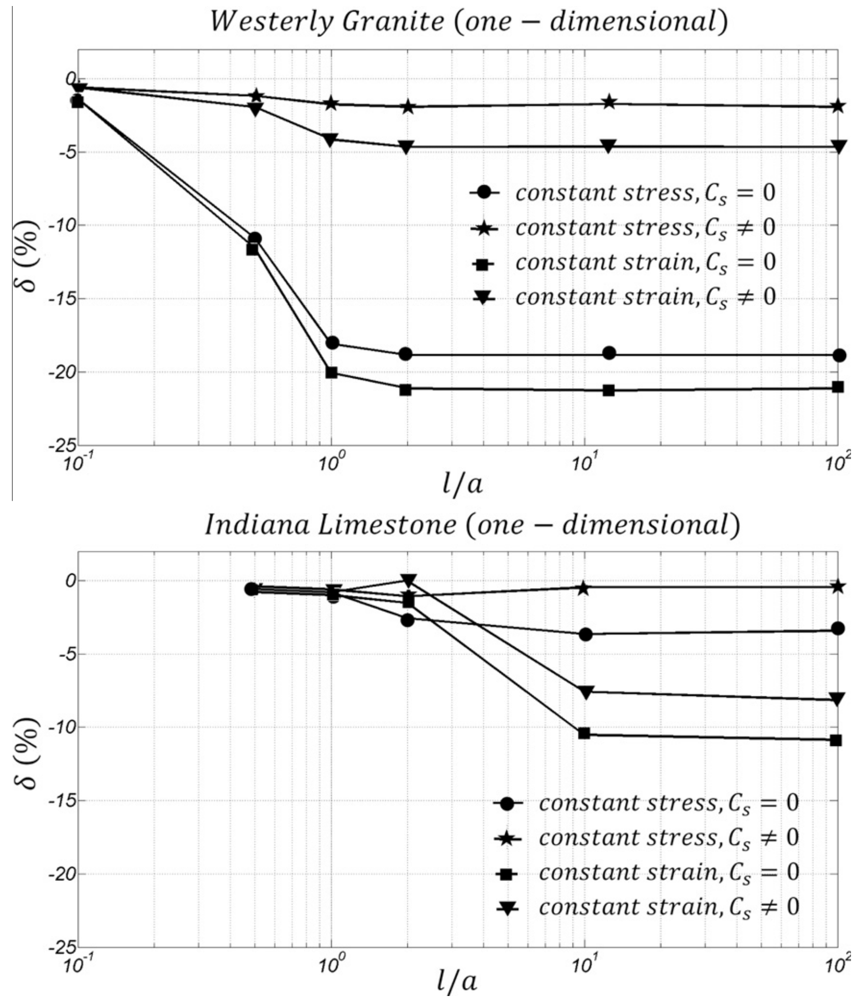


**Fig. 8.** Comparison of the computational results obtained from Biot poroelasticity equations with the piezo-conduction equation for one-dimensional constant stress and constant strain hydraulic pulse testing for different aspect ratios.

### *5.1. Radial flow hydraulic pulse testing*

Radial flow hydraulic pulse testing involves the application of a pressure pulse to a central cavity drilled into the rock specimen. The sample was vacuum saturated for a period of 7 days to ensure that the pore space was saturated. There are no assurances that the entire pore space would be saturated but experience from previous experimental investigations involving cement grouts [16], Barre Granite [17] and Indiana Limestone [19] using such techniques have resulted in reliable results concerning saturation. The plane surfaces of the hollow cylinder were sealed with an epoxy to ensure that the flow pattern corresponds to radial flow. A schematic view of the experimental faculty is shown in Fig. 10. It consists of a test frame to provide a seal between the centrally cored Stanstead Granite specimen and a stainless steel "permeameter" that has a water inflow, an outlet and a connection to a pressure transducer. This arrangement is similar to the devices used by Selvadurai and Carnaffan [16] when performing hydraulic pulse tests on cementitious grout and by Selvadurai and Selvadurai [45] when performing steady state patch permeability tests. The permeameter has provisions for extracting air from the central cavity that could influence the performance of the hydraulic pulse test. Fig. 11 shows the details of the permeameter.

The procedure for performing the radial flow pulse test involves a preliminary test that is performed on a hollow aluminum cylinder to test the efficiency of seals used to maintain radial flow. In these trial tests, the cavity in the aluminum cylinder should maintain the pressure with negligible decay (0.5% pressure decay in 2000 s and 7% decay in 50,000 s). The sealing is achieved through a set of O-rings located between the permeameter and the epoxy-covered surface of a hollow aluminum cylinder. Radial flow pulse tests were performed by subjecting the central cavity to a pressure pulse that is applied for a duration of less than 60 s. This time interval can be regarded as representative of a hydraulic pressure pulse of a delta function-type. Fig. 12 shows the results for time-dependant pressure decay obtained during 10 pulse tests conducted on the Stanstead Granite. The interpretation of pulse tests for estimating the permeability can be performed in a variety of ways and the most convenient procedure is to develop a set of pulse decay curves that can be used to "bound" the value of permeability. The bounding procedure for obtaining a range of values for $K$ is considered to be more realistic than obtaining a specific value. The bounding data was determined from three different approaches: (i) the conventional piezo-conduction equation analyses ($K_{pc}$), (ii) the conventional piezo-conduction equation analyses, which also accounts for the compressibility of grains ($K_{pcc}$), and (iii) a fully coupled analysis of the radial flow pulse decay problem ($K_{fc}$). The bounding curves shown in Fig. 12 are only estimations based on the approach (i) while Table 3 summarizes the permeability ranges estimated from all three methods. There are only marginal differences between the three estimates.

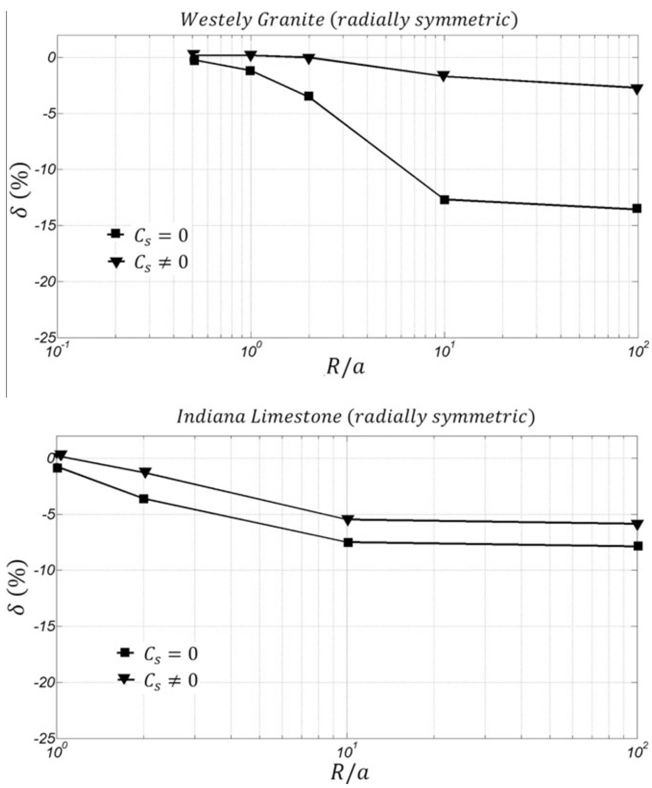


**Fig. 9.** Comparison of the computational results obtained from Biot poroelasticity equations with the piezo-conduction equation for radially symmetric hydraulic pulse testing for different aspect ratios.

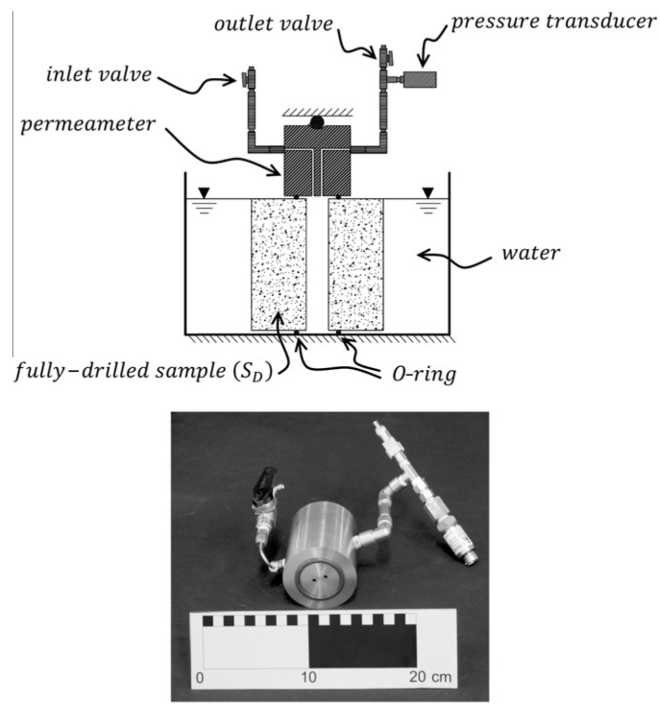


**Fig. 11.** Components of the permeameter used to perform hydraulic pulse tests on fully drilled samples.

### 5.2. Patch pulse test

We next consider the problem of pulse loading applied at a patch located on the plane surface of a cylinder of Stanstead Granite. The patch pulse tests have been successfully used for estimating the permeability characteristics of rocks such as Berea Sandstone [46] and Indiana Limestone [45]. Here we present an application that investigates transient behavior of a hydraulic pulse applied at a circular opening located at the axis of the sealed plane surface of a cylindrical sample of Stanstead Granite. The sealing between the permeameter and the granite cylinder is achieved by applying an axial stress of 1.5 MPa. The pressure pulses applied within the opening are kept to a maximum of 150 kPa to eliminate any leakage at the sample–rubber gasket interface. The procedure adapted to constrain the gasket during its compression is similar to that used by Selvadurai and Selvadurai [45] and has provided a successful sealing technique. A schematic view of the test arrangement is shown in Fig. 13. The annular region of the plane surface of the cylinder is maintained in a sealed and submerged condition and initially a vacuum is applied to remove any trapped air. The residual pore pressure fields created during saturation of the sample under vacuum are allowed to dissipate over a 7 day period. The

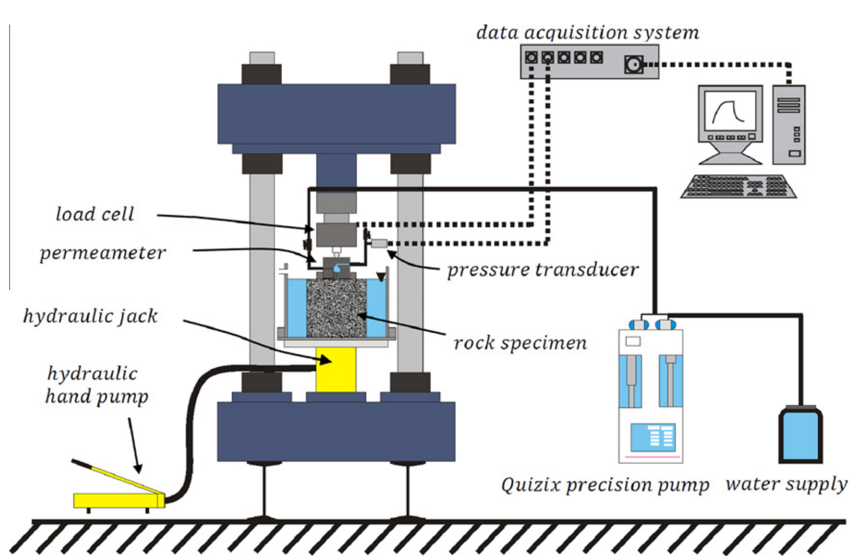


**Fig. 10.** Experimental faculty for measuring the permeability of low permeability geomaterials.

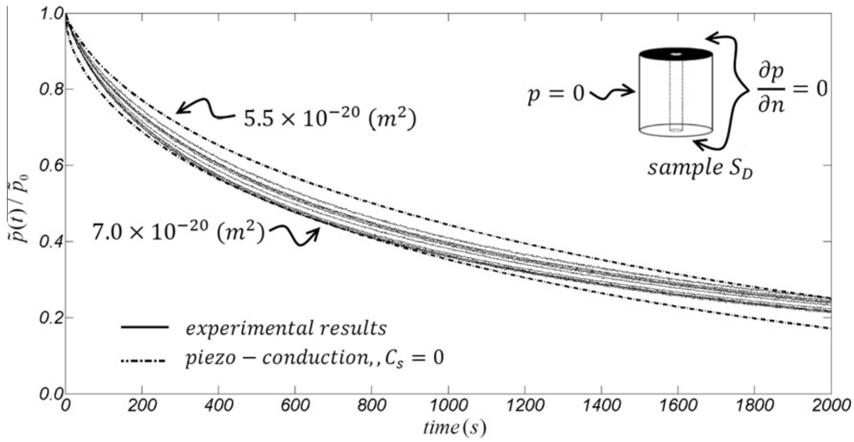


**Fig. 12.** Results of hydraulic pulse tests performed on a fully drilled Stanstead Granite cylinder (sample $S_D$). The analysis of data was done using the piezo-conduction equation and neglecting the compressibility of the solid grains.

**Table 3**
Permeability values for Stanstead Granite.

| Sample | $K_{fc}$ (m$^2$) | $K_{pcc}$ (m$^2$) | $K_{pc}$ (m$^2$) |
|---|---|---|---|
| $S_U$ | $(1.2–1.7) \times 10^{-20}$ | $(1.2–1.7) \times 10^{-20}$ | $(1.1–1.6) \times 10^{-20}$ |
| $S_D$ | $(6.0–7.7) \times 10^{-20}$ | $(6.0–7.7) \times 10^{-20}$ | $(5.5–7.0) \times 10^{-20}$ |

fluid cavity is subjected to a pressure pulse to initiate the pulse tests. Fig. 14 shows the results of surface pulse tests derived from 10 tests conducted on the cylindrical sample. These results have been interpreted on the basis of the three sets of permeability estimates obtained in Section 5.1. The pore pressure boundary condition applicable to the patch pulse testing that uses the piezo-conduction equation analysis (with and without influences of grain compressibility) is shown in Fig. 15(a) and the pore pressure, displacement and traction boundary condition needed

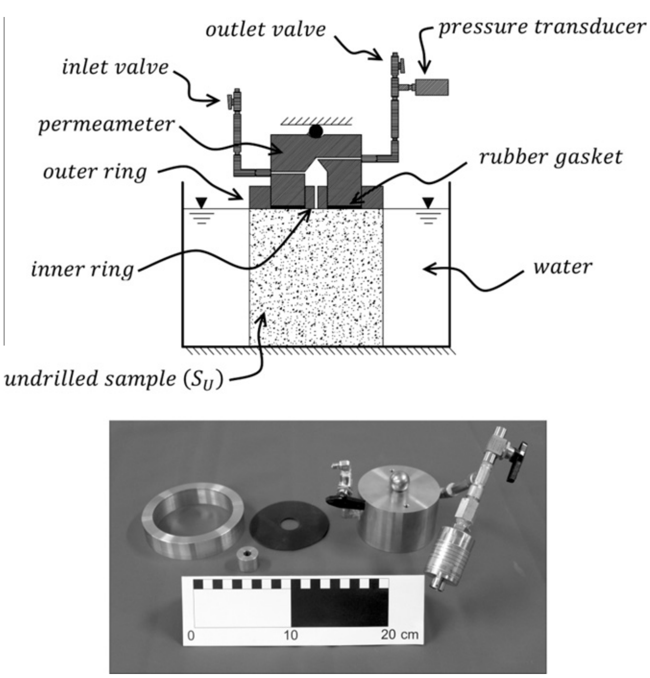


**Fig. 13.** Components of the permeameter used to perform hydraulic pulse tests on undrilled samples.

to perform a fully coupled analysis are shown in Fig. 15(b). The results derived from the three sets of theoretical estimates for the permeability predicted the correct trends for the pulse decay, although the numerical predictions show deviation from the experimental data. The likely causes for the discrepancies are not readily evident. The likely causes for the discrepancies seen between the experimental observations and theoretical predictions for the patch pulse tests could be due to several factors including leakage, damage during sample fabrication, dissolved air and transverse isotropy influences of permeability. The first two factors can be eliminated since this would have resulted in faster decay rates than those presented in Fig. 14. Air entrapment in the system was minimized through vacuum saturation protocols that were also adopted for the purely radial flow pulse tests. The presence of permeability transverse isotropy could be a likely cause for a less than perfect correlation in the pulse decay results. There is little information on the estimation of permeability anisotropy of the Stanstead Granite. Literature on fracture toughness testing suggests the presence of some anisotropy in the fracture toughness properties [47]. As a parametric exercise, hydraulic pulse test behavior was modeled with hydraulic transverse isotropy maintaining the range of values of the radial hydraulic conductivity estimated from the purely radial flow tests. It is estimated that the permeability in the axial direction should be 20 times smaller than the permeability in the radial direction in order to achieve a correlation between the computational predictions provided by the fully coupled analysis and the experimental data. This conclusion, however, requires further study.

## 6. Concluding remarks

In this paper, the range of applicability of the piezo-conduction equation used for estimating the hydraulic properties of low permeability rocks was examined using Biot's poroelasticity theory. The results indicate that the prediction for the pressure decay can be influenced by both the model used to interpret the test and the test configuration; this in turn can influence the interpretation of the permeability of the porous medium. The conventional modeling of the test that uses the piezo-conduction equation does not account for the compressibility of the solid grains and this factor can have an influence on the estimation of the permeability of geomaterials with small Biot coefficients. A further consideration is the influence of generalized deformations of the porous skeleton; this can be accommodated for by modeling the piezo-conduction equation by appeal to Biot's classical theory of poroelasticity. The

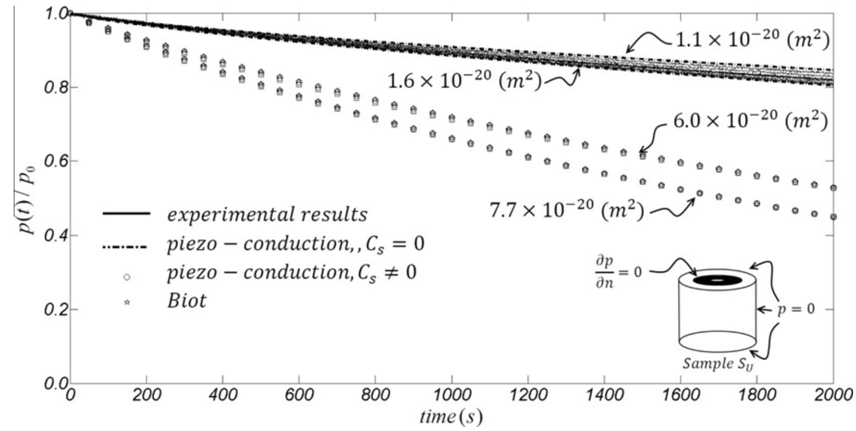


**Fig. 14.** Results of hydraulic pulse tests performed on an undrilled Stanstead Granite cylinder (sample $S_U$). The analysis of data was done using the piezo-conduction equation and neglecting the compressibility of the solid grains.

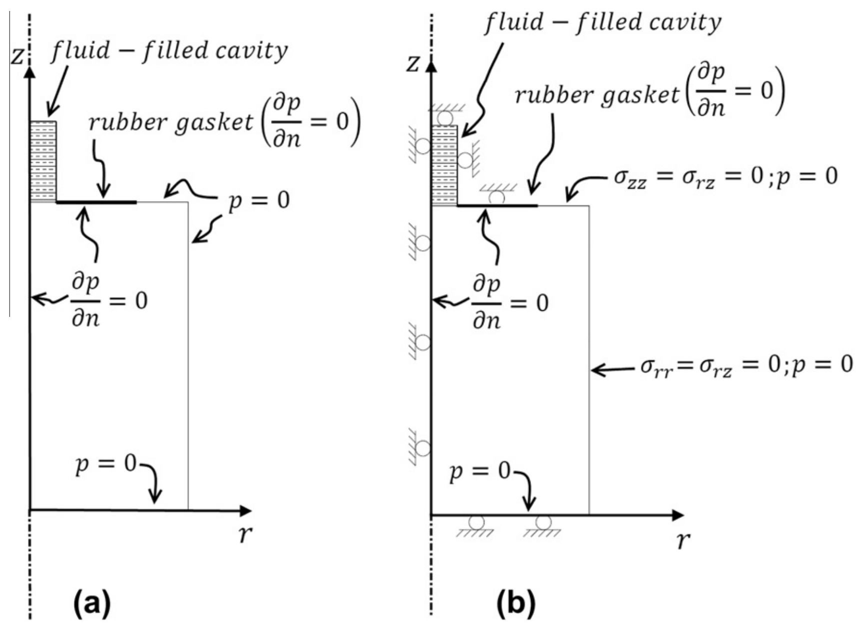


**Fig. 15.** Sample $S_U$: (a) geometry and boundary conditions used for the piezo-conduction equation and (b) geometry and boundary conditions used for Biot's poroelasticity equations.

incorporation of the generalized deformations can also influence the interpretation of test results. The performance of the two modeling techniques is demonstrated by examining the pulse decay observed in two typical geologic media that have been investigated in the literature. Finally, the results of hydraulic pulse tests performed on two Stanstead Granite samples were analyzed by employing the separate approaches. Comparisons show that, although the permeability obtained from different approaches change, the order of magnitude is consistent for the performed tests. Also, the computational studies performed show that the choice of a modeling technique influences one-dimensional hydraulic pulse test analysis more than radially symmetric test configurations. In general, the most complete approach to analyze the hydraulic pulse test results is to use Biot's poroelasticity theory, which accounts for deformability of the solid grains and models the coupled interaction of porous skeleton deformation and pressure change. This technique, however, is complicated and time consuming to employ. For simplicity, the permeability parameter can be estimated using the piezo-conduction equation that accounts for grain compressibility.

## Acknowledgments

The work reported in the paper was supported by a NSERC Discovery Grant and a NSERC Strategic Grant awarded to the first author. The authors are indebted to the reviewers for their constructive comments that lead to substantial improvements in the presentation.

## References

[1] Brace W, Walsh J, Frangos WT. Permeability of granite under high pressure. J Geophys Res 1968;73(6):2225–36.
[2] Bear J. Dynamics of fluid in porous media. New York: American Elsevier; 1972.
[3] Barenblatt GI, Entov VM, Ryzhik VM. Theory of fluid flows through natural rocks. Dordrecht: Kluwer Academic Publishers; 1990.
[4] Phillips OM. Flow and reactions in permeable rocks. Cambridge: Cambridge University Press; 1991.
[5] Selvadurai APS. Partial differential equations in mechanics, vol. 1: fundamentals, Laplace's equation, diffusion equation, wave equation. Berlin: Springer; 2000.
[6] Zoback MD, Byerlee JD. The effect of microcrack dilatancy on the permeability of Westerly Granite. J Geophys Res 1975;80(5):752–5.

[7] Trimmer D, Bonner B, Heard HC, Duba A. Effect of pressure and stress on water transport in intact and fractured gabbro and granite. J Geophys Res 1980;85(B12):7059–71.
[8] Hsieh PA, Tracy JV, Neuzil CE, Bredehoeft JD, Silliman SE. A transient laboratory method for determining the hydraulic properties of tight rocks – I. Theory. Int J Rock Mech Min Sci Geomech Abstr 1981;18(3):245–52.
[9] Neuzil C, Cooley C, Silliman SE, Bredehoeft JD, Hsieh PA. A transient laboratory method for determining the hydraulic properties of tight rocks – II. Application. Int J Rock Mech Min Sci Geomech Abstr 1981;18(3):253–8.
[10] Selvadurai APS, Letendre A, Hekimi B. Axial flow hydraulic pulse testing of an argillaceous limestone. Environ Earth Sci 2011;64:2047–58.
[11] Song I, Renner J. Linear pressurization method for determining hydraulic permeability and specific storage of a rock sample. Geophys J Int 2006;164(3):685–96.
[12] Cooper HH, Bredehoeft JD, Papadopulos IS. Response of a finite diameter well to an instantaneous charge of water. Water Resour Res 1967;3(1):263–9.
[13] Papadopulos SS, Bredehoeft JD, Cooper HH. On the analysis of slug test data. Water Resour Res 1973;9(4):1087–9.
[14] Bredehoeft JD, Papadopulos SS. A method for determining the hydraulic properties of tight formations. Water Resour Res 1980;16(1):233–8.
[15] Detournay E, Cheng AHD. Poroelastic response of a borehole in a non-hydrostatic stress field. Int J Rock Mech Min Sci Geomech Abstr 1988;25(3):171–82.
[16] Selvadurai APS, Carnaffan P. A transient pressure pulse method for the measurement of permeability of a cement grout. Can J Civ Eng 1997;24(3):489–502.
[17] Selvadurai APS, Boulon M, Nguyen TS. The permeability of an intact granite. Pure Appl Geophys 2005;162(2):373–407.
[18] Selvadurai APS, Jenner L. Radial flow permeability testing of an argillaceous Limestone. Ground Water 2012. http://dx.doi.org/10.1111/ (ISSN) 1745-6584.
[19] Selvadurai APS. Influence of residual hydraulic gradients on decay curves for one-dimensional hydraulic pulse tests. Geophys J Int 2009;177(3):1357–65.
[20] Biot M. General theory of three-dimensional consolidation. J Appl Phys 1941;12(2):155–64.
[21] Walder J, Nur J. Permeability measurement by the pulse decay method: effect of poroelastic phenomena and nonlinear pore pressure diffusion. Int J Rock Mech Min Sci Geomech Abstr 1986;23(3):225–32.
[22] Hart DJ, Wang HF. Poroelastic effects during a laboratory transient pore pressure test. In: Thimus JF, Abousleiman Y, Cheng AHD, Coussy O, Detournay E, editors. Poromechanics. Rotterdam: Balkema; 1998. p. 579–82.
[23] Wang H. Theory of linear poroelasticity with applications to geomechanics and hydrogeology. Princeton: Princeton University Press; 2000.
[24] Rice JR, Cleary MP. Some basic stress diffusion solutions for fluid-saturated elastic porous media with compressible constituents. Rev Geophys 1976;14(2):227–41.
[25] Coussy O. Mechanics of porous continua. Chichester: John Wiley; 1995.
[26] Lewis RW, Schrefler BA. The finite element method in the static and dynamic deformation and consolidation of porous media. Chichester: John Wiley; 1998.
[27] Detournay E, Cheng AHD. Fundamentals of poroelasticity. In: Hudson JA, editor. Comprehensive rock engineering. New York: Pergamon Press; 1993.
[28] Scheidegger AE. Flow through porous media. Appl Mech Rev 1960;13:313–8.
[29] Paria G. Flow of fluids through porous deformable solids. Appl Mech Rev 1963;6:901–7.
[30] Selvadurai APS, editor. Mechanics of poroelastic media. Dordrecht: Kluwer Academic Publishers; 1996.
[31] Selvadurai APS. The analytical method in geomechanics. Appl Mech Rev 2007;60(3):87.
[32] de Boer R. Porous media: theory and experiments. Dordrecht: Kluwer Academic Publishers; 1999.
[33] Schanz M. Poroelastodynamics: linear models, analytical solutions, and numerical methods. Appl Mech Rev 2009;62(3):030803.
[34] Selvadurai APS, Suvorov A. Application of the COMSOL Multiphysics code for coupled thermo-hydro-mechanical modelling relevant to deep geologic repositories. Nuclear Waste Management Office Report NWMO TGS-509, ON, Canada; 2010.
[35] Selvadurai APS, Suvorov A. Boundary heating of poroelastic and poro-elastoplastic spheres. Proc Roy Soc Math Phys Sci Ser A 2012;468(2145):2779–806.
[36] Selvadurai APS, Suvorov A, Selvadurai PA. Application of the COMSOL Multiphysics code for coupled thermo-hydro-mechanical modeling of fractured rock mass subjected to glaciation Loads. Nuclear Waste Management Office Report NWMO TGS-510, ON, Canada; 2011.
[37] Carslaw HS, Jaeger JC. Conduction of heat in solids. London: Oxford University Press; 1959.
[38] Mandel J. Consolidation des sols (étude mathématique). Géotechnique 1953;3:287–99.
[39] Cryer RW. A comparison of three dimensional theories of Biot and Terzaghi. Q J Mech Appl Mech 1963;16:401–12.
[40] Gibson RE, Knight K, Taylor PW. A critical experiment to examine theories of three-dimensional consolidation. In: Proceedings of the European conference on soil mechanics and foundation engineering, vol. 1, Wiesbaden; 1963. p. 69–76.
[41] Selvadurai APS, Shirazi A. Mandel–Cryer effects in fluid inclusions in damage susceptible poro-elastic media. Comput Geotech 2004;37:285–300.
[42] Lecampion A, Constantinescu A, Malinsky. Identification of poroelastic constants of tight rocks from laboratory tests. Int J Geomech 2006;6:201–8.
[43] Iqbal MJ, Mohanty B. Experimental calibration of ISRM suggested fracture toughness measurement techniques in selected brittle rocks. Rock Mech Rock Eng 2007;40(5):453–75.
[44] White FM. Fluid mechanics. New York: McGraw-Hill; 1986.
[45] Selvadurai APS, Selvadurai PA. Surface permeability tests: experiments and modelling for estimating effective permeability. Proc Roy Soc A: Math Phys Sci 2010;466(2122):2819–46.
[46] Tidwell VC, Wilson JL. Laboratory method for investigating permeability upscaling. Water Resour Res 1997;33(7):1607–16.
[47] Nasseri MHB, Grasselli G, Mohanti B. Fracture toughness and fracture roughness in anisotropic granitic rocks. Rock Mech Rock Eng 2010;43:403–15.